

Weak localization and spin splitting in inversion layers on *p*-type InAs

Christopher Schierholz,* Toru Matsuyama, Ulrich Merkt, and Guido Meier

Institut für Angewandte Physik und Zentrum für Mikrostrukturforschung, Universität Hamburg, Jungiusstrasse 11, D-20355 Hamburg, Germany

(Received 2 August 2004; published 21 December 2004)

We report on the magnetoconductivity of quasi-two-dimensional electron systems in inversion layers on *p*-type InAs single crystals. In low magnetic fields pronounced features of weak localization and antilocalization are observed. They are almost perfectly described by the theory of Iordanskii, Lyanda-Geller, and Pikus. This allows us to determine the spin splitting and the Rashba parameter of the ground electric subband as a function of the electron density.

DOI: 10.1103/PhysRevB.70.233311

PACS number(s): 72.20.Fr, 72.25.Rb

The multitude of new applications promised by use of the electron's spin as a degree of freedom in addition to its charge has led to growing interest in the area of spintronics.¹ For semiconductor based spintronics, the required control of the electron spin is expected to be achieved via spin-orbit interaction. In single crystals this interaction originates from two terms: the bulk inversion asymmetry of the crystal lattice² and the structure inversion asymmetry.³ The latter term includes contributions from the electric field and from the boundary conditions and is commonly called Rashba term. For many heterostructures good agreement between calculated Rashba parameters and experimentally deduced values is reached.^{4,5} In the case of two-dimensional electron systems (2DES) in surface inversion layers the spin-orbit interaction and the Rashba parameter are still under debate.^{6–8}

Theoretical considerations^{9,10} have shown that the Rashba term is the main cause of the spin splitting of electric subbands in InAs structures. This is supported by the experiments of Luo *et al.* on InAs quantum wells.¹¹ It has been demonstrated for various heterostructures^{4,12,13} as well as for inversion layers on *p*-type InAs single crystals⁶ that the Rashba term can be influenced by an external gate voltage. This was concluded from beating patterns in Shubnikov-de Haas (SdH) oscillations at various gate voltages. However, contrary to SdH experiments, all proposed spintronic devices operate at zero or low magnetic fields. Calculations by Lommer *et al.* showed that not only the magnitude but even the sign of the spin splitting can change between low and high magnetic fields for AlGaAs/GaAs heterostructures.⁹ For spintronic applications it is thus necessary to determine the spin splitting at near-zero magnetic fields.

Dresselhaus *et al.*¹⁴ showed that the destruction of weak antilocalization by small magnetic fields can be used to determine the strength of the spin-orbit interaction in GaAs. These authors analyzed their data with the theory of Hikami, Larkin, and Nagaoka.¹⁵ Kawaguchi *et al.*¹⁶ found that this theory could not correctly reproduce the weak antilocalization observed in inversion layers on *p*-type InAs. Koga *et al.*⁵ showed that a quantitative description of weak antilocalization in InAlAs/InGaAs/InAlAs heterostructures is possible with the model developed by Iordanskii, Lyanda-Geller, and Pikus (ILP).^{17,18} Analyses of weak antilocalization using ILP theory have been performed on AlGaAs/AlInAs quantum wells,¹⁸ AlGaAs/GaAs *p*-type quantum wells,¹⁹ and

AlInAs/GaInAs/AlInAs quantum wells.⁵ However, this approach so far has not been used to analyze the magnetoconductance of 2DES on bulk narrow-gap semiconductors.

We have performed measurements on Zn doped *p*-type InAs (100) single crystals with an acceptor concentration of approximately $N_A = 2 \times 10^{17} \text{ cm}^{-3}$. Band bending leads to a 2DES confined in the approximately triangular asymmetric potential well characteristic of a natural surface inversion layer.²⁰ The narrow band gap of InAs results in strong spin-orbit interaction, with the Rashba term that originates from the asymmetry of the potential well dominating the spin splitting of the electric subbands.⁹ Our samples are field-effect transistors in Corbino geometry. The electrodes are defined by optical lithography and deposited by thermal evaporation. They consist of 35 nm thick aluminum passivated by 10 nm of gold. The entire structure is covered by a 340 nm thick SiO₂ insulator onto which a gate covering the semiconductor channel is patterned. All measurements are performed in lock-in technique at a temperature of 2.65 K in a ⁴He cryostat.

The measured magnetoconductances show strong parabolic signatures as can be seen for fields above 300 mT in Fig. 1(a). This classical Drude magnetoconductivity $G(B) = G_0(1 + \mu^2 B^2)^{-1}$ stems from the Corbino geometry

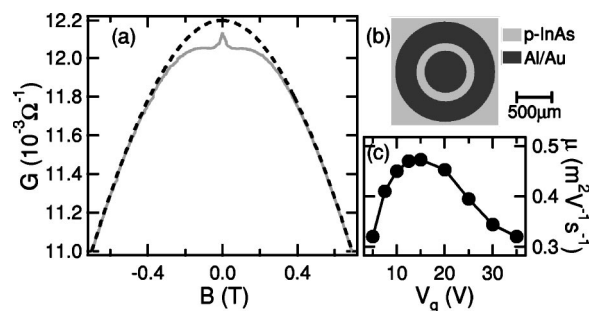


FIG. 1. (a) Experimental magnetoconductance for a gate voltage of $V_g = 15$ V at $T = 2.65$ K (solid line) as well as a calculated Drude parabola (dashed line). (b) Schematic of the sample geometry. The radius of the inner electrode is $300 \mu\text{m}$, the channel length $100 \mu\text{m}$, and the radius of the outer electrode $700 \mu\text{m}$. (c) Electron mobility versus gate voltage.

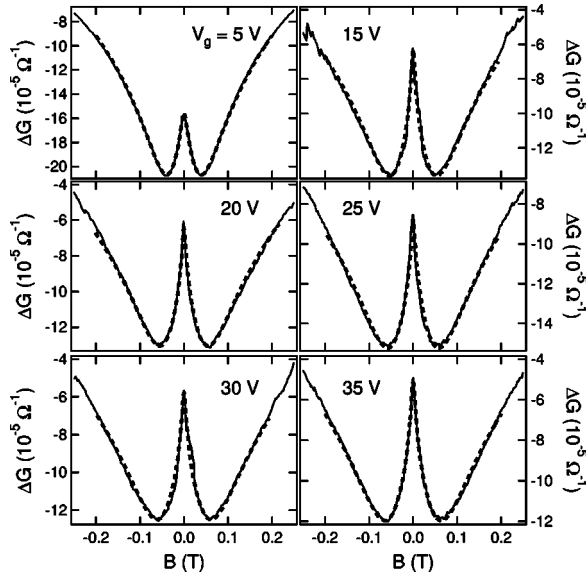


FIG. 2. Experimental magnetoconductances recorded at 2.65 K for various gate voltages (solid lines). The classical Drude conductance is subtracted. Theoretical conductances (dashed lines) are calculated from the theory of Iordanskii, Lyanda-Geller, and Pikus (Refs. 17 and 18).

depicted in Fig. 1(b). A parabola fit to the experimental data yields the zero-field conductivity G_0 as well as the electron mobility μ . The mobility as a function of the applied gate voltage is shown in Fig. 1(c). It is characteristic for a metal-oxide-semiconductor (MOS) transistor: surface scattering at low gate voltages and ionized impurity scattering at high gate voltages lead to reduced mobilities.²⁰ The inversion threshold of the sample lies at a gate voltage of $V_g \cong 1.8$ V. The total electron density n_s is determined from SdH oscillations of the source-drain resistance. We find a linear dependence $n_{s,\uparrow/\downarrow} [\text{cm}^{-2}] = 1.46 \times 10^{11} + 6.70 \times 10^{10} V_g [\text{V}]$ on the gate voltage.

The Drude parabola is subtracted from the magnetoconductance to leave the quantum corrections originating from weak localization and antilocalization remaining. Starting from zero-field, these corrections at first exhibit a negative magnetoconductance originating from spin-orbit interaction based weak antilocalization followed by a positive magnetoconductance due to weak localization. Figure 2 shows results for various gate voltages. The conductance corrections $\Delta G(B)$ are fit according to the ILP theory which provides an excellent description. Considering the structure inversion asymmetry as dominant origin of the zero-field spin splitting in our system and thus neglecting the bulk inversion asymmetry ($\Omega_3=0$ in Refs. 17 and 18), only the characteristic magnetic fields of inelastic and of spin-orbit scattering,

$$H_\phi = \frac{\hbar}{4De\tau_\phi} \text{ and } H_{\text{SO}} = \frac{\Delta_0^2 \tau_{\text{tr}}}{8\hbar De} = \frac{1}{8\hbar^3 e \pi} \frac{(m^* \Delta_0)^2}{n_s} \quad (1)$$

are relevant in the fitting procedure.¹⁸ In these relations D is the diffusion coefficient, τ_ϕ and τ_{tr} are the inelastic and transport relaxation times, respectively, and Δ_0 is the spin-splitting energy in zero magnetic field. The characteris-

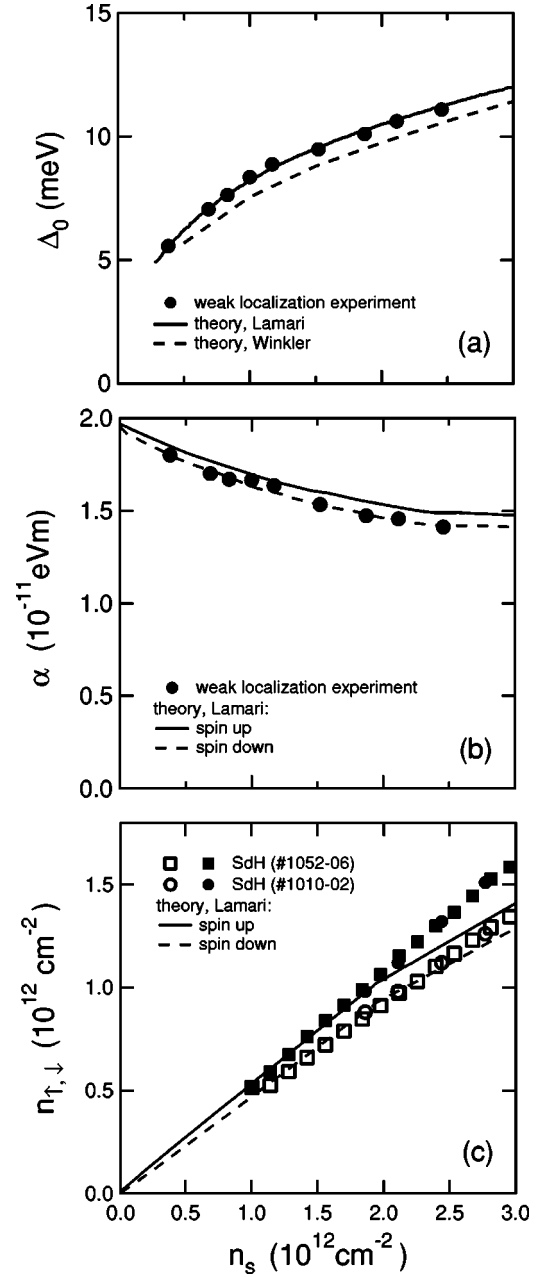


FIG. 3. (a) Spin-splitting energy at the Fermi level. Theoretical data are taken from Lamari (Ref. 22) and Winkler (Ref. 23). (b) Rashba parameter. Dashed and solid lines are calculated for the spin-split subbands at the Fermi level (Ref. 22). (c) Occupation of the spin-split subbands. Open and closed symbols are data for spin-down and spin-up states of the two different samples indicated by circles and squares. Theoretical curves are taken from Lamari (Ref. 7).

tic field H_{tr} of transport scattering can be ignored in the fit as it only results in a shift in $\Delta G(B)$.^{5,18} The diffusion coefficient is given by $D = \tau_{\text{tr}} v_F^2 / 2$ with the Fermi velocity $v_F = \hbar k_F / m^*$, the Fermi wave vector k_F , and the electron effective mass m^* .

We calculate the zero-field spin splitting Δ_0 from Eq. (1) and the Rashba parameter from the relation⁵

$$\alpha = \frac{\sqrt{\hbar^3 e H_{\text{SO}}}}{m^*}. \quad (2)$$

Note that only the absolute value of the Rashba parameter can be determined, not its sign. In the case of inversion layers we do not expect a change of sign as their asymmetric surface potentials do not change their overall shape. The analysis is performed for the effective mass m^* of the ground electric subband at the Fermi energy. For high carrier densities n_s this mass is determined from temperature dependent SdH oscillations. At the inversion threshold the band edge mass of the ground subband of $m_0^* = 0.026 \cdot m_e$ is used.²¹ Hence we find

$$m^* = (0.026 + 0.012 \times 10^{-12} n_s - 0.001 \times 10^{-24} n_s^2) \cdot m_e, \quad (3)$$

with the electron density n_s in units of cm^{-2} .

Figure 3(a) shows the carrier-density dependence of the spin-splitting energy Δ_0 . The splitting increases monotonically with the electron density n_s and is in good agreement with band-structure calculations^{7,22,23} displayed in the same figure. The Rashba spin-orbit parameter α is shown in Fig. 3(b). The analysis of weak localization experiments with the ILP theory yields one Rashba parameter for each carrier density. Band-structure calculations yield different Rashba parameters for the two spin subbands because of the slight difference between the Fermi wave vectors for spin-up and spin-down states. However, this difference is small and can be neglected in the comparison with the weak localization data. A decrease of the Rashba parameter with increasing carrier density is observed. Again, the experimental results are in good agreement with the values obtained from the calculations. Figure 3(c) shows the occupations of the spin-split subbands as determined from SdH oscillations.^{6,24} At carrier densities below $2.0 \times 10^{12} \text{ cm}^{-2}$ a good agreement between theory and experiment is observed. The first excited subband is only populated for carrier densities above about $2.3 \times 10^{12} \text{ cm}^{-2}$.²⁵ In the theory for a doping concentration of $1.8 \times 10^{17} \text{ cm}^{-3}$, population of the first excited subband occurs for carrier densities above $2.0 \times 10^{12} \text{ cm}^{-2}$, leading to kinks in the plots. This can be seen most easily in Fig. 3(c) for the spin-up electrons.

Values of the Rashba parameter determined from SdH oscillations in high magnetic fields^{6,24} do not agree with the multiband calculations of Lamari^{7,22} and Winkler²³ and the

results from weak localization reported here. While they are of the same order of magnitude, they increase with increasing carrier density.

Using the effective mass from Eq. (3) and the subband carrier densities of Lamari displayed in Fig. 3(c) the simple relation²⁵ $\alpha = \hbar^2 [\sqrt{4\pi n_\uparrow} - \sqrt{4\pi n_\downarrow}] / m^*$ yields Rashba parameters that agree well with those in Fig. 3(b). Hence the effective mass cannot be responsible for the discrepancy between the results in low and high magnetic fields. We currently do not understand why the splitting of the spin-subband densities from SdH oscillations as well as the increase thereof with growing carrier density are larger than theoretically predicted.

The situation in heterostructures of low carrier density is different, as a good agreement between theory and high-field experiments is found.¹³ This indicates that the simple evaluation of beating patterns in SdH oscillations is not sufficient for the high carrier densities in 2DES inversion layers on *p*-type InAs crystals. In the carrier-density range well above 10^{12} cm^{-2} the spin-split energies no longer exhibit linear dispersion. Then band nonparabolicity and higher order terms in the expansion of the Rashba parameter become decisive. Hence it is important to consider the Rashba parameter as a function of both the electric field as well as of the in-plane wave vector.^{10,26} The wave vector dependence exceeds the electric field contribution at high electron densities and leads to a decrease of the Rashba parameter. Obviously, for inversion layers on *p*-type InAs the evaluation of the weak localization measurements provides more reliable values for the Rashba parameter than that of SdH oscillations.

To conclude, we have studied spin-orbit interaction in the surface inversion layer on *p*-type InAs single crystals using weak localization at near zero magnetic field. Excellent description of the experimental data could be achieved through the theory of Iordanskii, Lyanda-Geller, and Pikus.^{17,18} We find the carrier-density dependence of the spin-splitting energy Δ_0 and the Rashba parameter α of the ground electric subband to be in very good agreement with multiband calculations, but to differ from previous analyses in which SdH beating patterns were evaluated.

We thank Saadi Lamari and Roland Winkler for valuable discussions and for providing detailed theoretical data, and Alexander Thieme for software development. The authors gratefully acknowledge financial support from the BMBF via the Verbundprojekt 13N8281 and from the Deutsche Forschungsgemeinschaft via SFB 508.

*Electronic address: cschierh@physnet.uni-hamburg.de

¹S. A. Wolf, D. D. Awschalom, R. A. Buhrman, J. M. Daughton, S. von Molnár, M. L. Roukes, A. Y. Chtchelkanova, and D. M. Treger, *Science* **294**, 1488 (2001).

²G. Dresselhaus, *Phys. Rev.* **100**, 580 (1955).

³Yu. A. Bychkov and E. I. Rashba, *J. Phys. C* **17**, 6039 (1984).

⁴D. Grundler, *Phys. Rev. Lett.* **84**, 6074 (2000).

⁵T. Koga, J. Nitta, T. Akazaki, and H. Takayanagi, *Phys. Rev. Lett.*

89, 046801 (2002).

⁶T. Matsuyama, R. Kürsten, C. Meißner, and U. Merkt, *Phys. Rev. B* **61**, 15 588 (2000).

⁷S. Lamari, *Phys. Rev. B* **64**, 245340 (2001).

⁸P. Pfeffer and W. Zawadzki, *J. Supercond.* **16**, 351 (2003).

⁹G. Lommer, F. Malcher, and U. Rössler, *Phys. Rev. Lett.* **60**, 728 (1988).

¹⁰E. A. de Andrada e Silva, G. C. La Rocca, and F. Bassani, *Phys.*

- Rev. B **50**, 8523 (1994).
- ¹¹J. Luo, H. Munekata, F. F. Fang, and P. J. Stiles, Phys. Rev. B **38**, 10 142 (1988); **41**, 7685 (1990).
- ¹²J. Nitta, T. Akazaki, H. Takayanagi, and T. Enoki, Phys. Rev. Lett. **78**, 1335 (1997).
- ¹³G. Engels, J. Lange, Th. Schäpers, and H. Lüth, Phys. Rev. B **55**, R1958 (1997).
- ¹⁴P. D. Dresselhaus, C. M. A. Papavassiliou, R. G. Wheeler, and R. N. Sacks, Phys. Rev. Lett. **68**, 106 (1992).
- ¹⁵S. Hikami, A. Larkin, and Y. Nagaoka, Prog. Theor. Phys. **63**, 707 (1980).
- ¹⁶Y. Kawaguchi, I. Takayanagi, and S. Kawaji, J. Phys. Soc. Jpn. **56**, 1293 (1987).
- ¹⁷S. V. Iordanskii, Y. B. Lyanda-Geller, and G. E. Pikus, JETP Lett. **60**, 206 (1994).
- ¹⁸W. Knap, C. Skierbiszewski, A. Zduniak, E. Litwin-Staszewska, D. Bertho, F. Kobbi, J. L. Robert, G. E. Pikus, F. G. Pikus, S. V. Iordanskii, V. Mosser, K. Zekentes, and Yu. B. Lyanda-Geller, Phys. Rev. B **53**, 3912 (1996).
- ¹⁹S. Pedersen, C. B. Sørensen, A. Kristensen, P. E. Lindelof, L. E. Golub, and N. S. Averkiev, Phys. Rev. B **60**, 4880 (1999).
- ²⁰T. Ando, A. B. Fowler, and F. Stern, Rev. Mod. Phys. **54**, 437 (1982).
- ²¹U. Merkt and S. Oelting, Phys. Rev. B **35**, 2460 (1987).
- ²²S. Lamari, Phys. Rev. B **67**, 165329 (2003).
- ²³R. Winkler (private communication).
- ²⁴Ch. Schierholz, R. Kürsten, G. Meier, T. Matsuyama, and U. Merkt, Phys. Status Solidi B **233**, 436 (2002).
- ²⁵R. Kürsten, Ph.D. thesis, Universität Hamburg, 2002 (ISBN 3-89873-388-2). The spin-splitting of the first excited subband is of the same order of magnitude as that of the ground subband.
- ²⁶E. A. de Andrada e Silva, G. C. La Rocca, and F. Bassani, Phys. Rev. B **55**, 16 293 (1997).